



Research Paper

Profiling of glucose degradation products through complexation with divalent metal ions coupled with ESI/qTOF/MS/MS analysis

Eun Sil Kim, Varoujan Yaylayan^{*}

Department of Food Science and Agricultural Chemistry, McGill University, 21111 Lakeshore, Ste Anne de Bellevue, Quebec, H9X 3V9, Canada



ARTICLE INFO

Keywords:

Sugar iron complexes

Qualitative profiling of sugar degradation products

ESI/qTOF/MS

ABSTRACT

Sugar degradation products generated through thermal treatment of foods are considered the key precursors for various flavor compounds, toxicants and browning, but their high reactivity makes their detection difficult. In this study, a convenient analytical procedure for profiling of various reactive sugar intermediates having enediol or α -dicarbonyl moieties through complexation with divalent metal ions combined with electrospray ionization/quadrupole time-of-flight mass spectrometry was developed. Excess divalent iron chloride (FeCl_2) was added to glucose or $^{13}\text{U6}$ -[glucose] solutions in methanol either before or after heating at 110°C for 2 h, and the samples were analyzed by tandem mass spectrometry. The results indicated the formation of ethylene glycol, glycolaldehyde, glyceraldehyde, glycerol, methylglyoxal, glyoxylic acid, erythrose, erythrosone, 3-deoxy-erythrosone, erythritol, ribose, ribosone, 3-deoxy-ribose, ribitol, 3-deoxy-glucosone, and rhamnose. These sugars and sugar degradation products acting as bidentate ligands were detected as positively charged mono- and bis-sugar iron complexes in the form of $[\text{M} + \text{H}]^+$, $[\text{M} + \text{Na}]^+$, $[\text{M} + \text{K}]^+$, $[\text{M} + \text{Fe}^{35}\text{Cl}]^+$, and $[\text{M} + \text{Fe}^{37}\text{Cl}]^+$, as well as by charge localization on iron $[\text{M}]^+$. The divalent metal complexation technique was applied for the profiling of sugar degradation products in aged manuka honey.

1. Introduction

During the thermal treatment of food, reducing sugars undergo a complex reaction cascade that leads to the formation of various reactive sugar intermediates and degradation products such as α -dicarbonyl, α -hydroxy-carbonyl, deoxyosones, and α -hydroxy acids (Davidek et al., 2006a). In the context of the Maillard reaction, these intermediates constitute the “sugar fragmentation pool” that provides important precursors necessary for the formation of heterocyclic aromatic compounds (Yaylayan, 1997). Some of these reactive sugar intermediates form independently through acid- or base-catalyzed sugar degradation reactions, while others form interactively through reactions with amino acids or proteins. The ability to profile such reaction mixtures for reactive sugar intermediates or sugar degradation products (SDP) poses a considerable analytical challenge due to their high reactivity and transient nature, which allows them to form and react before detection. Although there are numerous quantitative analytical techniques based on chemical derivatization using silylating agents (Davidek et al., 2006a; Yaylayan, 1997; Zheng et al., 2019; Davidek et al., 2006b; Usui et al., 2007; Paravisini & Peterson, 2019). There are no methods reported so far for the fast detection of such sugar degradation products. Chemical

derivatization is usually employed in conjunction with various chromatographic and mass spectrometric techniques such as gas chromatography mass spectrometry (GC/MS) and liquid chromatography mass spectrometry (LC/MS) (Page & Conacher, 1982). Taking advantage of the ease of complexation of divalent metal ions such as copper (II) (Nashalian & Yaylayan, 2015) with not only α -dicarbonyl compounds but also with many of the shorter-chain sugar fragments formed during the Maillard reaction, and their subsequent stabilization, we propose the utilization of divalent metal ions as suitable fast trapping agents for profiling of such reactive SDP as metal complexes in conjunction with electrospray ionization/quadrupole time-of-flight mass spectrometry (ESI/qTOF/MS) analysis.

2. Materials and methods

2.1. Materials and reagents

Iron(II) chloride (FeCl_2) (99%) and D-glucose were purchased from Sigma-Aldrich Chemical Co. (Oakville, Ontario, Canada). $[\text{U6-}^{13}\text{C}]$ glucose (99%) was purchased from Cambridge Isotope Laboratories (Andover, MI). Liquid chromatography-mass spectrometry (LC-MS)

^{*} Corresponding author.E-mail address: varoujan.yaylayan@mcgill.ca (V. Yaylayan).

grade methanol (OmniSolv, > 99%) was obtained from VWR International (Mississauga, Ontario, Canada). Manuka honey used in this study was purchased from a local store in 2009 and aged at room temperature.

2.2. Sample preparation

Test model systems were prepared by adding FeCl₂ (6.4 mg) either before or after heating glucose (18 mg) in methanol (1 mL) using sealed stainless-steel reactors at 110 °C for 2 h followed by evaporation of the solvent at 75 °C for 5 min. The samples were kept frozen until analysis. To see the effect of storage temperatures on the profile, the same samples were also stored for 15 days at room and at refrigerated temperatures.

Control model systems were prepared by heating glucose (18 mg) in methanol (1 mL) at 110 °C for 2 h without the addition of FeCl₂ or by adding FeCl₂ (6.4 mg) to an unheated glucose (18 mg) in methanol (1 mL). Aged manuka honey (2 mg) was dissolved in methanol (2 mL) and then FeCl₂ (0.02 mg) was added and analyzed after storage at refrigerated conditions for 15 days. All samples were analyzed at least in two replicates as indicated in Table 1.

2.3. ESI/qTOF/MS analysis

The dry reaction mixtures were dissolved in liquid chromatography (LC)-grade methanol to a concentration of 1 mg/mL. The samples were then diluted 10-fold in 10% methanol prior to analysis by ESI/qTOF/MS in positive mode. The ESI/qTOF/MS system was comprised of a Bruker Maxis Impact quadrupole-time-of-flight mass spectrometer (Bruker Daltonics, Bremen, Germany) operated in positive-ion mode. This system was permitted a high resolution with ~60,000 full sensitivity resolution and mass accuracy of 1 ppm. Samples (1 µL) were injected directly into ESI/qTOF/MS. Instrument calibration was performed using sodium formate clusters. The electrospray interface settings were the following: nebulizer pressure, 0.6 bar; drying gas, 4 L/min; temperature, 180 °C; and capillary voltage, 4500 V. The scan range was from *m/z* 100 to 1000. Molecular formulae were assigned to all the observed peaks based on their exact *m/z* values by using the online software “ChemCalc” (Institute of Chemical Sciences and Engineering, Lausanne, Switzerland) (Patiny & Borel, 2013). ESI/qTOF/MS/MS was carried out in multiple reaction monitoring (MRM) mode using 20.0 eV collision energy for the ions at *m/z* 270, 284, and 295.

2.4. Structural elucidation

Evidence for the proposed structures of SDP was provided through ESI/qTOF/MS analysis of their elemental composition, MS/MS and through isotope-labeling studies using ¹³C-U6 glucose, in addition the

proposed structures were based on the well-known glucose degradation products. Furthermore, the incorporation of chlorine from FeCl₂ in the identified complexes was confirmed through detection of the isotopic signature of chlorine at *M* + 2 peaks *ca.* 25% relative intensity of *M* ion. Isotope labelling techniques was used to confirm the elemental composition and the MS/MS fragmentation mechanisms using corresponding isotopically labelled counterparts generated from ¹³C-U6 labelled glucose.

The proposed structures represent only one possible isomer or stereoisomer out of many possible for a particular nominal molecular weight. Those structures are the most commonly reported in the literature.

3. Results and discussion

To develop a convenient technique for profiling SDP formed during the Maillard reaction or thermal processing of foods, a method based on the known and observed ease of complexation of Maillard reaction intermediates with divalent metal ions (Nashalian & Yaylayan, 2015) was investigated using FeCl₂. In this study, glucose was degraded by heating at 110 °C for 2 h in methanol and excess FeCl₂ was added either before ([Glu/FeCl₂]) or after the degradation reaction ([Glu]/FeCl₂) and analyzed using ESI/qTOF/MS. Heated glucose in the absence of FeCl₂ was also analyzed ([Glu]) as a control (see Table 1). The control system without addition of the metal salt did not display any detectable low-molecular-weight SDP in the positive ionization mode. All other model systems, however, generated metal complexes with various sugar fragments, which are listed in Table 2 (see also Figs. S1 and S2). In these model systems, the glucose degradation products acted as bidentate ligands and were detected as positively charged mono- and bis-sugar iron complexes such as [M + H]⁺, [M + Na]⁺, [M + K]⁺, [M + Fe³⁵Cl]⁺, and [M + Fe³⁷Cl]⁺ in addition to charge localization on iron [M]⁺ (see Fig. 1). Moreover, some of the ions were associated with more than one solvent molecule (water and methanol), and some also showed dehydration products. The data indicated that the iron(II) complexes were stable enough to be detected by MS. The iron in these complexes assumed different charged states of 0, +1, and +2 depending on the number and type of bonding (covalent or coordinate) and simultaneously formed up to four bonds, two covalent and two coordinate, allowing for the binary complexes to be detected as protonated, sodiated, chlorinated, or potassiumated ions as shown in Fig. 1.

3.1. Profiling of glucose degradation products via Iron(II) complexation as determined by ESI/qTOF/MS and ESI/qTOF/MS/MS

ESI/qTOF/MS analysis (positive ionization mode) of the different model systems listed in Table 1, indicated that in the absence of metal salts, only few low-molecular-weight SDP and some high-molecular-weight products in addition to unreacted glucose could be positively

Table 1
Composition of the model systems studied.^a

Model System-	
Control Model Systems	Glucose solution heated in the absence of FeCl ₂ kept at room temperature (RT) for 15 days until analyzed - [Glu] ^b
Test Model Systems	FeCl ₂ added to a glucose solution at RT analyzed after storage at RT for 15 days - Glu/FeCl ₂ FeCl ₂ added to heated glucose solution kept in the freezer for 15 days until analyzed - [Glu] FeCl ₂ I FeCl ₂ added to heated glucose solution kept at RT for 15 days until analyzed - [Glu] FeCl ₂ II Glucose solution heated in the presence of FeCl ₂ kept at RT for 15 days until analyzed - [Glu/FeCl ₂]
Food Model Systems	Methanolic manuka honey solution was kept in the refrigerator for 15 days until analyzed - Honey FeCl ₂ was added to a methanolic solution of manuka honey and kept in the refrigerator for 15 days until analyzed - Honey/FeCl ₂

^a All model systems were analyzed minimum in two replicates.

^b Square brackets indicate heating at 110 °C for 2 h in methanol by using sealed stainless-steel reactors.

Table 2
Observed SDP following the method of complexation with FeCl₂ ^a.

	SDP ^b of glucose	SDP in aged manuka
C2	Ethylene Glycol and Glycolaldehyde	Not detected
C3	Glycerol, Glyceraldehyde and Methylglyoxal	Glyceraldehyde
C4	Erythrose, 3-Deoxyerythrose, 3-Deoxyerythrose, Erythrosone, and Erythritol	Erythrose, 3-Deoxyerythrosone, 3-Deoxyerythrose, Erythrosone, and Erythritol
C5	Ribose, Ribosone, 3-Deoxyribosone, 3-Deoxypentosulose, and Ribitol	Ribose, Ribosone, and 3-Deoxyribosone
C6	3-Deoxyglucosone, Glucosone, 3,4-Dideoxyglucosone, and Rhamnose	3-Deoxyglucosone

^a See Table S1 for their various mono-, bis(sugar) metal complexes and hydrates observed (reported names represent the most common isomer).

^b Dehydrated and methanolated counterparts are not listed (see Table S1).

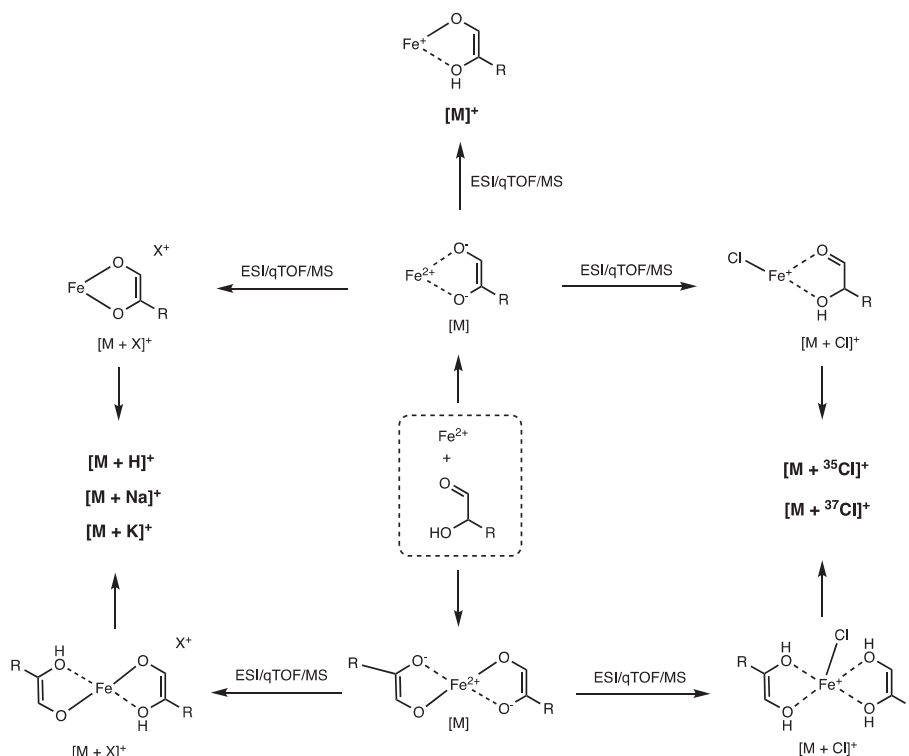


Fig. 1. SDP can form single and/or bis-(1,2-enediol) complexes of iron (II) and can be detected through various ionizations processes to form positively charged species such as $[M]^+$, $[M + H]^+$, $[M + Na]^+$, $[M + K]^+$, $[M + ^{35}Cl]^+$, and $[M + ^{37}Cl]^+$. The 1, 2-dicarbonyl type degradation products can also form single or bis-(1,2-dicarbonyl) iron complexes of the type $[M + ^{35}Cl]^+$ and $[M + ^{37}Cl]^+$ (Not shown).

charged and detected (see Figs. S1 and S2). However, in the model systems with metal ions, enhanced intensity of the SDP was observed due to their complexation with the metal ions (see Table S1). This can be attributed to the increased stability of the metal complexes versus free SDP. These complexes can prevent their decomposition/polymerization and at the same time can provide structural features (see Fig. 1) that are lacking in SDP for the development and stabilization of positive charges necessary for their detection under positive ionization mode of ESI-qTOF/MS system.

Storing the samples at room temperature before analysis did not significantly alter their sugar degradation profile, although some enhanced peak intensities were observed in the room temperature stored samples but those were not statistically significant and were within the experimental error of calculated average peak intensities. Furthermore, room temperature storage may encourage binary complex formation between two SDP.

No new products were observed in $[Glu/FeCl_2]$ relative to $[Glu]/FeCl_2$. Only enhanced intensities of some peaks, indicating that heating the sample in the presence of $FeCl_2$ enhances the signals of low intensity degradation products, which can aid in their profiling. It is important to caution the formation of some low intensity sugar alcohols such as ethylene glycol, glycerol, erythritol, and ribitol as artifacts during this procedure (see section 3.2).

The detailed glucose degradation products listed in Table S1 were categorized below based on the number of sugar carbon atoms incorporated in the observed degradation products as confirmed by isotope labelling technique.

3.1.1. C2 sugar degradation products

Ethylene glycol and glycolaldehyde were categorized as C2 sugar fragments (see Table S1). The former was detected as $[M]^+$ at m/z 116.9638 ($C_2H_5FeO_2$), presumed to be formed by the reduction of glycolaldehyde (see section 3.2) which was observed as both $[M + Fe^{35}Cl]^+$ at m/z 150.9247 ($C_2H_4[^{35}Cl]FeO_2$) and $[M + Fe^{37}Cl]^+$ at m/z 152.922

($C_2H_4[^{37}Cl]FeO_2$). Both C2 SDP were detected in all the model systems, with higher peak intensities when samples were heated with $FeCl_2$.

3.1.2. C3 sugar degradation products

Glycerol, methylglyoxal, and glyceraldehyde were categorized as C3 sugar fragments (see Table S1). Glycerol was observed as iron(II) complex in the form of $[M]^+$ at m/z 146.9742 ($C_3H_7FeO_3$). Methylglyoxal, one of the most important 1,2-dicarbonyl compounds, was detected as a binary (enediol) iron(II) complex, was observed as $[M + Fe^{35}Cl]^+$ and $[M + Fe^{37}Cl]^+$ at m/z 234.9464 ($C_6H_8[^{35}Cl]FeO_4$) and m/z 236.9441 ($C_6H_8[^{37}Cl]FeO_4$) (see Fig. 1). The bis-methylglyoxal iron(II) complexes were observed in all the model systems. Glyceraldehyde was also observed in all the model systems as a mono-chlorinated iron complexes $[M + Fe^{35}Cl]^+$ and $[M + Fe^{37}Cl]^+$ at m/z 180.9355 ($C_3H_6[^{35}Cl]FeO_3$) and m/z 182.336 ($C_3H_6[^{37}Cl]FeO_3$), respectively, as well as charge localized iron complex $[M]^+$ at m/z 144.9585 ($C_3H_5FeO_3$).

3.1.3. C4 sugar degradation products

Various C4 SDP were observed including mono- and bis-3-deoxyerythrosone, erythrose, erythritol complexed with dehydrated erythrosone and iron, and hydrated erythrosone (see Table S1). Erythrose and its derivatives were detected as various mono and binary iron(II) complexes shown in Fig. 1 such as $[M + H]^+$, $[M + K]^+$, $[M + Na]^+$, $[M + Fe^{35}Cl]^+$, $[M + Fe^{37}Cl]^+$, and $[M]^+$. The 3-Deoxyerythrosone was conjugated with iron(II) in mono-, bis- and as methanolated 3-deoxyerythrosone iron(II) complexes.

Mono 3-deoxyerythrosone was observed at m/z 158.9743 ($C_4H_7FeO_3$) and its dehydration product was detected at m/z 158.9743 ($C_4H_5FeO_2$). It was also detected as $[M + Fe^{35}Cl]^+$ at m/z 194.9505 ($C_4H_8[^{35}Cl]FeO_3$) and $[M + Fe^{37}Cl]^+$ at m/z 196.9493 ($C_4H_8[^{37}Cl]FeO_3$) as shown in Table S1. Furthermore, 3-deoxyerythrosone was also detected as the potassiated dimer at m/z 300.9784 ($C_8H_{14}FeO_6$), and as well as the counter ligand in various complexes with other glucose degradation products such as glycolaldehyde at m/z 265.0019 ($C_7H_{13}FeO_7$), and

glyoxylic acid at m/z 280.9962 ($C_7H_{13}FeO_8$). The proposed erythrosone derivatives were further confirmed through isotope labelling technique which indicated the incorporation of four carbon atoms from [^{13}C -U6] glucose. Erythrose was observed in various charged states such as the ions at m/z 174.9694 ($C_4H_7FeO_4$) [$M + Fe^{35}Cl$] $^+$, m/z 210.9465 ($C_4H_8[^{35}Cl]FeO_4$), and [$M + Fe^{37}Cl$] $^+$ at m/z 212.9445 ($C_4H_8[^{37}Cl]FeO_4$). In addition, erythritol was detected as an artifact (see section 3.2) at m/z 176.9839 ($C_4H_9FeO_4$) and only in [Glu/ $FeCl_2$] model system. Erythrosone on the other hand, was detected in the monohydrated form at m/z 190.9645 ($C_4H_7FeO_5$) and as the counter ligand of a binary complex with erythritol observed at m/z 295.0119 ($C_8H_{15}FeO_8$), as well as its dehydration product [$M + H$] $^+$ at m/z 277.0015 ($C_8H_{13}FeO_7$).

The proposed binary complex observed at m/z 295.0119 ($C_8H_{15}FeO_8$) was further studied through analysis of its MS/MS fragmentations as shown in Table 3 and Fig. 2. The predicted erythrosone moiety at [M] $^+$ m/z 174.9685 was the base peak and erythritol appeared at m/z 234.9888 (51.4%). The proposed MS/MS fragmentation of the ion at m/z 295.0119 is shown in Fig. 3 and the structural information was based on the isotope labelling studies and MS/MS fragmentations. As shown in Table 3 both fragments incorporated four carbon atoms from glucose. The proposed mechanism of formation of erythritol is further discussed in section 3.2 below.

3.1.4. C5 sugar degradation products

The C5 SDP, ribose, ribosone, and dideoxypentosulose were observed in the form of mono- and binary iron(II) complexes (see Table S1). Ribose

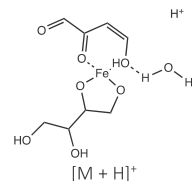
was detected as a mono iron(II) complex at m/z 204.9803 ($C_5H_9FeO_5$), and its dehydration reaction generated the ion at m/z 186.9696. In addition, the ribose binary iron (II) complex was found as [$M + H$] $^+$ at m/z 355.0334 ($C_{10}H_{19}FeO_{10}$), as well as its dehydration product [$M + H$] $^+$ at m/z 337.0228 ($C_{10}H_{17}FeO_9$). Ribosone and dideoxypentosulose were detected as their hydrated forms in all the model systems studied. Hydrated ribose was found at m/z 220.975 ($C_5H_9FeO_6$) and its dehydration product at m/z 202.9647 ($C_5H_7FeO_5$). The hydrated dideoxypentosulose was detected as [$M + ^{35}Cl$] $^+$ at m/z 224.9618 ($C_5H_{10}[^{35}Cl]FeO_4$), and as [$M + ^{37}Cl$] $^+$ at m/z 226.9594 ($C_5H_{10}[^{37}Cl]FeO_4$), the latter was also observed at m/z 188.9849 ($C_5H_9FeO_4$) and as its dehydration product at m/z 170.9743 ($C_5H_9FeO_4$). In terms of the reduced ribose adduct, ribitol, was detected at m/z 206.9956.

3.1.5. C6 sugar degradation products

The C6 SDP were observed as the most diversified species (see Table S1). The 3-deoxyglucosone was the dominant ion in all model systems in the form of various iron(II) complexes. In particular, it was associated with solvent molecules, water and/or methanol, and also afforded dehydration products. The dominant ion peaks were found at m/z 270.9677 and m/z 272.9648 corresponding to [$M + Fe^{35}Cl$] $^+$ ($C_6H_{12}[^{35}Cl]FeO_6$) and [$M + Fe^{37}Cl$] $^+$ ($C_6H_{12}[^{37}Cl]FeO_6$), respectively, and both underwent dehydration to generate ions at m/z 252.9569 as [$M + Fe^{35}Cl$] $^+$ ($C_6H_{10}[^{35}Cl]FeO_5$) and m/z 254.9543 as [$M + Fe^{37}Cl$] $^+$ ($C_6H_{10}[^{37}Cl]FeO_5$). Moreover, 3-deoxyglucosone was detected as a monohydrated iron (II) complex at m/z 234.9907 ($C_6H_{11}FeO_6$) and as

Table 3

MS/MS fragmentations of the ion at m/z 295 ($C_8H_{15}FeO_8$) generated in the [Glu/ $FeCl_2$] model system (see Figs. 2 and 3).

m/z 295	m/z	Intensity (%)	Elemental composition	Error PPM ^a	^{13}C -U6	Elemental composition	Error PPM
	174.9685 ^b	100	$C_4H_7FeO_4$	-4.97	4	$[^{13}C]_4H_7FeO_4$	-7.2
	234.9888	51.4	$C_4H_{12}FeNaO_6$	3.01	4	$[^{13}C]_4H_{12}FeNaO_6$	37.18
	295.0129	89.3	$C_8H_{15}FeO_8$	4.31	8	$[^{13}C]_8H_{15}FeO_8$	-6.49

^a Error (in ppm) in calculating the elemental composition.

^b Base peak.

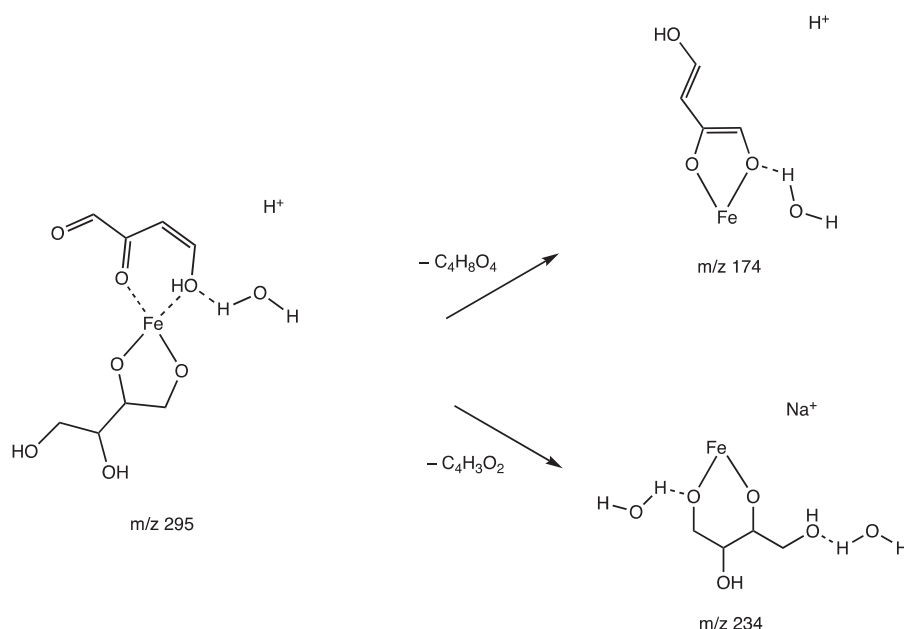


Fig. 2. Proposed ESI/qTOF/MS/MS fragmentations of the ion at m/z 295 observed in the [Glu/ $FeCl_2$] model system (see Table 3).

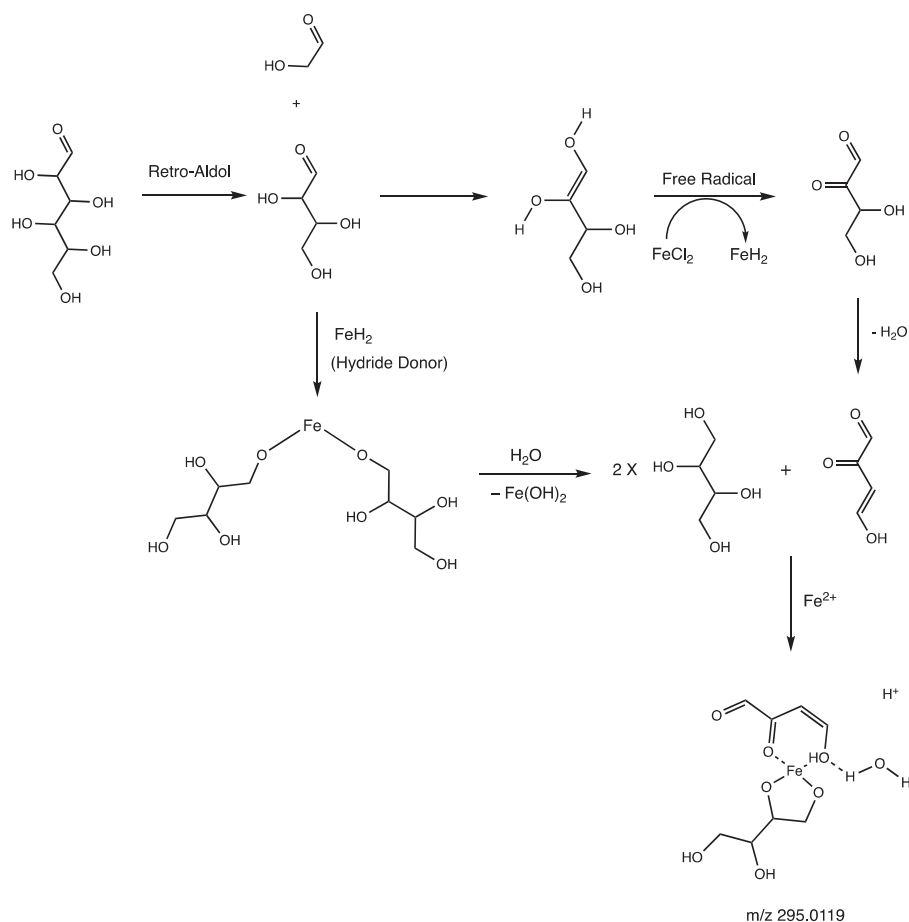


Fig. 3. Proposed mechanism of formation of erythritol detected as bis (sugar) iron(II) complex at m/z 295 (see Table 3 and Fig. 2).

dehydrated ion at m/z 216.9802 ($C_6H_{11}FeO_6$) and also as $[M - 2H_2O]^+$ at m/z 198.9695 ($C_6H_9FeO_5$). Furthermore, 3-deoxyglucosone was detected as chlorinated binary iron(II) complexes at m/z 451.032 ($C_{12}H_{24}[^{35}Cl]FeO_{12}$) and at m/z 453.0276 ($C_{12}H_{24}[^{37}Cl]FeO_{12}$), as well as $[M + H]^+$ at m/z 415.0548 ($C_{12}H_{23}FeO_{12}$) in addition to its dehydration products $[M + Fe^{35}Cl - H_2O]^+$ at m/z 433.0211 ($C_{12}H_{22}[^{35}Cl]FeO_{11}$) $[M + Fe^{37}Cl - H_2O]^+$ at m/z 435.0167 ($C_{12}H_{22}[^{37}Cl]FeO_{11}$) $[M + H - H_2O]^+$ at m/z 397.0445 ($C_{12}H_{21}FeO_{11}$), and $[M + H - 2H_2O]^+$ at m/z 379.0335 ($C_{12}H_{19}FeO_{10}$).

Mono- and bis-3-deoxyglucosone iron(II) complexes were also observed as various derivatives generated from further dehydration, hydration, and methanolation reactions as mentioned previously. Monomethanolated 3-deoxyglucosone was detected as $[M + Fe^{35}Cl]^+$ at m/z 284.9833 ($C_7H_{14}[^{35}Cl]FeO_6$) and $[M + Fe^{37}Cl]^+$ at m/z 286.9805 ($C_7H_{14}[^{37}Cl]FeO_6$). Monohydrated and methanolated 3-deoxyglucosone was found to form iron(II) complex at m/z 267.0169 ($C_7H_{15}FeO_7$), followed by dehydration steps to form two ions as $[M - H_2O]^+$ at m/z 249.0064 ($C_7H_{13}FeO_6$) and $[M - 2H_2O]^+$ at m/z 230.9951 ($C_7H_{11}FeO_5$). Dimethanolated adducts of 3-deoxyglucosone were also detected at m/z 317.0086 ($C_8H_{18}[^{35}Cl]FeO_7$). Methanolated 3-deoxyglucosone was also observed as binary iron (II) complexes associated with different sugar derivatives. For example, methanolated 3-deoxyglucosone conjugated with a hydrated 3-deoxyglucosone iron(II) complex was detected at m/z 465.0476 ($C_{13}H_{26}[^{35}Cl]FeO_{12}$) and at m/z 467.0432 ($C_{13}H_{26}[^{37}Cl]FeO_{12}$), along with its dehydration products at m/z 447.0364 ($C_{13}H_{24}[^{35}Cl]FeO_{11}$) and at m/z 449.0334 ($C_{13}H_{24}[^{37}Cl]FeO_{11}$), respectively. Bis-methanolated 3-deoxyglucosone was also observed at m/z 479.063 ($C_{14}H_{28}[^{35}Cl]FeO_{12}$), m/z 481.057 ($C_{14}H_{28}[^{37}Cl]FeO_{12}$), and m/z 443.0862 ($C_{14}H_{27}FeO_{12}$). Hydrated 3-deoxyglucosone associated with hydrated glucosone as iron(II) complex was also detected at m/z

453.0297 ($C_{12}H_{22}FeNaO_{13}$) with its dehydration product observed at m/z 435.0201 ($C_{12}H_{20}FeNaO_{12}$). Finally, rhamnose was observed as an iron complex conjugated with glycolaldehyde at m/z 309.0276 ($C_9H_{17}FeO_8$).

3.1.6. Comparison of the MS/MS fragmentations of the hydrated (m/z 270) and methanolated (m/z 284) 3-deoxyglucosone iron complexes using 20 eV collision energy

The difference between these two sugar iron complexes is the presence of non-covalently attached solvent molecules, and it is expected that their MS/MS fragmentations to be very similar as shown in Table 4 and in Fig. S3. The data has indeed indicated that in these molecules, 3-deoxyglucosone can be regenerated by the loss of water or methanol as shown in Fig. S3, which then can undergo further degradation to form reactive C2, C3, C4, and C5 sugar intermediates. These results are consistent with the proposed structure of these ions.

3.2. Formation of sugar alcohols as artifacts through redox reaction promoted by FeCl₂

In this procedure sugar alcohol intermediates such as ethylene glycol, glycerol, erythritol, and ribitol were observed as artifacts of using FeCl₂. Of particular interest was the ion observed at $[M + H]^+ = 295$. ESI/qTOF/MS/MS analysis of this ion indicated it was composed of iron complex of erythritol and dehydrated erythrosone as shown in Fig. 3. A proposed mechanism of formation of erythritol is shown in Fig. 3. According to this figure FeCl₂ through free radical mechanism can oxidize erythrose into erythrosone and in the process be converted into iron hydride (FeH₂), the latter, can reduce erythrose into erythritol through hydride transfer mechanism. Iron hydroxide [Fe(OH)₂] which is the predicted by-product of this reaction was observed in the reaction mixtures at $[M + H]^+ =$

Table 4
Comparison of elemental composition and accurate masses of product ions of m/z 270.9663 and m/z 284.9883 generated in MRM mode using 20 eV collision energy.

Product ions of <i>m/z</i> 270.9663						Product ions of <i>m/z</i> 284.9883					
<i>m/z</i>	Elemental composition	Error PPM ^a	¹³ C–U6	Elemental composition ^b	Intensity (%)	<i>m/z</i>	Elemental composition	Error PPM	¹³ C–U6	Elemental composition	Intensity (%)
127.0388	C ₆ H ₇ O ₃	−5.66	6	[¹³ C] ₆ H ₇ O ₃	16	127.0395	C ₆ H ₇ O ₃	−0.15	6	[¹³ C] ₆ H ₇ O ₃	10.6
145.0492	C ₆ H ₉ O ₄	−6.09	6	[¹³ C] ₆ H ₉ O ₄	23.4						
150.9243	C ₂ H ₄ [³⁵ Cl] FeO ₂	−4.1	2	[¹³ C] ₂ H ₄ [³⁵ Cl] FeO ₂	18.5	150.9237	C ₂ H ₄ [³⁵ Cl] FeO ₂	−8.07	2	[¹³ C] ₂ H ₄ [³⁵ Cl] FeO ₂	24.7
						158.9742	C ₄ H ₇ FeO ₃	−1.61	4	[¹³ C] ₄ H ₇ FeO ₃	11.7
162.969	C ₃ H ₇ FeO ₄	−2.27	3	[¹³ C] ₃ H ₇ FeO ₄	7.8						
168.9346	C ₂ H ₆ [³⁵ Cl] FeO ₃	−5.23	2	[¹³ C] ₂ H ₆ [³⁵ Cl] FeO ₃	40.3	168.935	C ₂ H ₆ [³⁵ Cl] FeO ₃	−2.86	2	[¹³ C] ₂ H ₆ [³⁵ Cl] FeO ₃	49.7
174.9685	C ₄ H ₇ FeO ₄	−4.97	4	[¹³ C] ₄ H ₇ FeO ₃	15.2	174.9689	C ₄ H ₇ FeO ₄	−2.69	4	[¹³ C] ₄ H ₇ FeO ₃	10.7
						176.984	C ₄ H ₉ FeO ₄	−5.76	nd ^d	nd	16.1
180.9347	C ₃ H ₆ [³⁵ Cl] FeO ₃	−4.33	3	[¹³ C] ₃ H ₆ [³⁵ Cl] FeO ₃	47.7	180.9344	C ₃ H ₆ [³⁵ Cl] FeO ₃	−5.99	3	[¹³ C] ₃ H ₆ [³⁵ Cl] FeO ₃	13.8
						184.9291	C ₂ H ₆ [³⁵ Cl] FeO ₄	−7.02	nd	nd	9.8
186.9684	C ₅ H ₇ FeO ₄	−5.19	5	[¹³ C] ₅ H ₇ FeO ₄	58.9						
192.9347	C ₄ H ₆ [³⁵ Cl] FeO ₃	−4.06	4	[¹³ C] ₄ H ₆ [³⁵ Cl] FeO ₃	21.5	192.9347	C ₄ H ₆ [³⁵ Cl] FeO ₃	−4.06	4	[¹³ C] ₄ H ₆ [³⁵ Cl] FeO ₃	16.1
198.9454 ^c	C ₃ H ₈ [³⁵ Cl] FeO ₄	−3.26	3	[¹³ C] ₃ H ₈ [³⁵ Cl] FeO ₄	100	198.9454	C ₃ H ₈ [³⁵ Cl] FeO ₄	−3.26	3	[¹³ C] ₃ H ₈ [³⁵ Cl] FeO ₄	15
204.9346	C ₅ H ₆ ClFeO ₃	−4.31	5	[¹³ C] ₅ H ₆ [³⁵ Cl] FeO ₃	7.6	198.9695	C ₆ H ₇ FeO ₄	0.65	6	[¹³ C] ₆ H ₇ FeO ₄	21
204.9792	C ₅ H ₉ FeO ₅	−3.58	5	[¹³ C] ₅ H ₉ FeO ₅	22.3						
210.9454	C ₄ H ₈ ClFeO ₄	−3.07	4	[¹³ C] ₄ H ₈ [³⁵ Cl] FeO ₄	57.2	210.9454 ^c	C ₄ H ₈ [³⁵ Cl] FeO ₄	−3.07	4	[¹³ C] ₄ H ₈ [³⁵ Cl] FeO ₄	100
						212.961	C ₄ H ₁₀ [³⁵ Cl] FeO ₄	−3.28	nd	nd	9.7
216.9792	C ₆ H ₉ FeO ₅	−3.39	6	[¹³ C] ₆ H ₉ FeO ₅	24.9	216.9793	C ₆ H ₉ FeO ₅	−2.93	6	[¹³ C] ₆ H ₉ FeO ₅	24.6
222.9452	C ₅ H ₈ [³⁵ Cl] FeO ₄	−3.8	5	[¹³ C] ₅ H ₈ ClFeO ₄ [*]	3.9						
228.9553	C ₄ H ₁₀ [³⁵ Cl] FeO ₅	−5.73	4	[¹³ C] ₄ H ₁₀ ClFeO ₅	25.7	228.9553	C ₄ H ₁₀ ClFeO ₅	−5.73	4	[¹³ C] ₄ H ₁₀ [³⁵ Cl] FeO ₅	45.3
234.9457	C ₆ H ₈ [³⁵ Cl] FeO ₄	−1.48	6	[¹³ C] ₆ H ₈ ClFeO ₄	10.5	234.9453	C ₆ H ₈ ClFeO ₄	−3.18	6	[¹³ C] ₆ H ₈ [³⁵ Cl] FeO ₄	13.1
234.9892	C ₆ H ₁₁ FeO ₆	−5.53	6	[¹³ C] ₆ H ₁₁ FeO ₆	26.7	234.9897	C ₆ H ₁₁ FeO ₆	−3.4	6	[¹³ C] ₆ H ₁₁ FeO ₆	36.7
252.9558	C ₆ H ₁₀ [³⁵ Cl] FeO ₅	−3.21	6	[¹³ C] ₆ H ₁₀ ClFeO ₅	84	252.956	C ₆ H ₁₀ ClFeO ₅	−2.42	6	[¹³ C] ₆ H ₁₀ [³⁵ Cl] FeO ₅	70.9
270.9663	C ₆ H ₁₂ [³⁵ Cl] FeO ₆	−3.24	6	[¹³ C] ₆ H ₁₂ ClFeO ₆	77.9	270.9667	C ₆ H ₁₂ ClFeO ₆	−1.76	6	[¹³ C] ₆ H ₁₂ [³⁵ Cl] FeO ₆	26.5
						284.9823	C ₇ H ₁₄ ClFeO ₆	−1.85	6	C[¹³ C] ₆ H ₁₄ [³⁵ Cl] FeO ₆	53.8

^a Error (in ppm) in calculating the elemental composition.
^b Error in the calculation of elemental formulas (¹³C–U6) ranged between 1.23 and 8.15 ppm except for the ion indicated by asterisks where the error was 12.63 ppm.
^c Base peak.
^d nd: not detected.

90.9475 with elemental composition H₃FeO₂ (−8.1 ppm error).

3.3. Detection of SDP in aged manuka honey

To confirm the applicability of this fast detection technique in profiling SDP in processed food, manuka honey was chosen as an example. Manuka honey is known to contain various SDP such as α -dicarbonyl compounds (Yan et al., 2019; Marceau & Yaylayan, 2009). Manuka honey was diluted in methanol and mixed with FeCl₂ as indicated in the experimental section and analyzed without heating by ESI/qTOF/MS. Most of the SDP identified in aged manuka honey were also reported in the literatures (Marceau & Yaylayan, 2009; Silva et al., 2016). Various reactive sugar intermediates with different charge localizations were observed in the manuka honey model system, and the detected metal complexes conjugated with SDP from three to six carbons in length are discussed below and listed in Table S2 and Table 2.

3.3.1. C3 sugar degradation products

Glyceraldehyde, the only C3 sugar fragment observed in the manuka honey, was detected at m/z 144.958 (C₃H₅FeO₃) and at m/z 180.9354 (C₃H₆[³⁵Cl]FeO₃).

3.3.2. C4 sugar degradation products

Eythrose, 3-deoxythrosone, 3-deoxyerythrose, erythritol, and dehydrated erythrosone were observed as C4 sugar degradation products. Erythrose, 3-deoxythrosone, and 3-deoxyerythrose were found as mono iron(II) complexes in the form of [M]⁺ at m/z 174.9683 (C₄H₇FeO₄), m/z 156.9598 (C₄H₅FeO₃), and m/z 158.975 (C₄H₇FeO₃). Erythritol was detected as a conjugated complex with dehydrated erythrosone at m/z 295.0095 (C₈H₁₅FeO₈). The details of this ion were discussed above.

3.3.3. C5 sugar degradation products

Ribosone and ribose were observed as the only C5 SDP. Ribosone was detected as a mono iron complex at m/z 202.9633 (C₅H₇FeO₅). Ribose was found as both mono- and binary iron(II) complexes at m/z 204.9785 (C₅H₉FeO₅) and at m/z 355.0307 (C₁₀H₁₉FeO₁₀) including its dehydration product at m/z 337.0228 (C₁₀H₁₇FeO₉).

3.3.4. C6 sugar degradation products

The 3-deoxyglucosone was detected in the form of mono- and binary iron(II) complexes. Mono-3-deoxyglucosone iron complexes were observed at m/z 270.9658 (C₆H₁₂[³⁵Cl]FeO₆), m/z 272.9635 (C₆H₁₂[³⁷Cl]

FeO₆) and m/z 234.9891 (C₆H₁₁FeO₆), along with their dehydration products such as [M + Fe³⁵Cl – H₂O]⁺ at m/z 252.9551 (C₆H₁₀[³⁵Cl]FeO₅) [M + Fe³⁷Cl – H₂O]⁺ at m/z 254.9561 (C₆H₁₀[³⁷Cl]FeO₅) [M – H₂O]⁺ at m/z 216.9786 (C₆H₁₁FeO₆), and [M – 2H₂O]⁺ at m/z 198.9679 (C₆H₉FeO₄). The bis-(3-DG) hydrated iron complex was detected at m/z 451.0275 (C₁₂H₂₄[³⁵Cl]FeO₁₂) and at m/z 453.0196 (C₁₂H₂₄[³⁷Cl]FeO₁₂), along with their dehydration products at m/z 433.018 (C₁₂H₂₂[³⁵Cl]FeO₁₁) and at m/z 415.0514 (C₁₂H₂₃FeO₁₂). The 3-deoxyglucosone associated peaks were present at relatively high intensities in the honey model system, followed by ribose adducts and C4 sugar fragments.

4. Conclusion

Reactive SDP acting as bidentate ligands were converted into stable metal complexes and were easily detected by electrospray ionization/quadrupole time-of-flight mass spectrometry in the positive ion mode. Formation of metal complexes prevented the degradation or polymerization of these reactive SDP and at the same time provided structural features (see Fig. 1) that were lacking in the free SDP for the development and stabilization of positive charges necessary for their detection under positive ionization mode of ESI-qTOF/MS system.

Author contributions

Eun Sil Kim: Data curation, Formal analysis, Methodology, Validation, Writing-original draft.

Varoujan Yaylayan: Supervision, Conceptualization, Project administration, Reviewing-Editing, and Funding acquisition.

Declaration of competing interest

The authors declare that they have no known competing financial interests or personal relationships that could have appeared to influence the work reported in this paper.

Acknowledgements

The authors acknowledge funding for this research from Natural Sciences and Engineering Research Council of Canada.

Appendix A. Supplementary data

Supplementary data to this article can be found online at <https://doi.org/10.1016/j.crfs.2020.10.001>.

Abbreviations

ESI/qTOF/MS	Electrospray Ionization Quadrupole Time-of-Flight Mass Spectrometry
MS/MS	Tandem Mass Spectrometry
SDP	Sugar degradation products
GC	Gas Chromatography
GC/MS	Gas Chromatography Mass Spectrometry
LC	Liquid Chromatography
LC/MS	Liquid Chromatography Mass Spectrometry

References

- Davidek, T., Robert, F., Devaud, S., Vera, F.A., Blank, I., 2006a. Sugar fragmentation in the maillard reaction cascade: formation of short-chain carboxylic acids, by a new oxidative α -dicarbonyl cleavage pathway. *J Agric Food Chem* 54, 6677–6684. <https://doi.org/10.1021/jf060668i>.
- Davidek, T., Robert, F., Devaud, S., Vera, F.A., Blank, I., 2006b. Sugar fragmentation in the maillard reaction cascade: isotope labeling studies on the formation of acetic acid by a hydrolytic β -dicarbonyl cleavage mechanism. *J Agric Food Chem* 54, 6667–6676. <https://doi.org/10.1021/jf060667q.s001>.
- Marceau, E., Yaylayan, V.A., 2009. Profiling of α -dicarbonyl content of commercial honeys from different botanical origins: identification of 3,4-Dideoxyglucosone-3-ene (3,4-DGE) and related compounds. *J Agric Food Chem* 57, 10837–10844. <https://doi.org/10.1021/jf903341t>.
- Nashalian, O., Yaylayan, V.A., 2015. Sugar-conjugated bis(glycinato)copper (II) complexes and their modulating influence on the maillard reaction. *J Agric Food Chem* 63, 4353–4360. <https://doi.org/10.1021/acs.jafc.5b00932>.
- Page, B.D., Conacher, B.S., 1982. The pros and cons of derivatization in the chromatographic determination of food additives. In: Frei, R.W. (Ed.), *Chemical derivatization in analytical chemistry*. Springer, US, pp. 243–292.
- Paravisini, L., Peterson, D.G., 2019. Reactive carbonyl species as key control point for optimization of reaction flavors. *Food Chem* 274, 71–78. <https://doi.org/10.1016/j.foodchem.2018.08.067>.
- Patiny, L., Borel, A. ChemCals, 2013. A building block for tomorrow's chemical infrastructure. *J Chem Inf Model* 53 (5), 1223–1228. <https://doi.org/10.1021/ci300563h>.
- Silva, P.M., Gauche, C., Gonzaga, L.V., Costa, A.C.O., Fett, R. Honey, 2016. Chemical composition, stability and authenticity. *Food Chem* 196, 309–323. <https://doi.org/10.3390/foods8110577>.
- Usui, T., Yanagisawa, S., Ohguchi, M., Yoshino, M., Kawabata, R., Kishimoto, J., Arai, Y., Watanabe, H., Hayase, F., 2007. Identification and determination of α -dicarbonyl compounds formed in the degradation of sugars. *Biosci Biotechnol Biochem* 71 (10), 2465–2472. <https://doi.org/10.1271/bbb.70229>.
- Yan, S., Sun, M., Zhao, L., Wang, K., Fang, X., Wu, L., Xue, X., 2019. Comparison of differences of α -dicarbonyl compounds between naturally matured and artificially heated Acacia honey: their application to determine honey quality. *J Agric Food Chem* 67 (46), 12885–12894. <https://doi.org/10.1021/acs.jafc.9b05484.s001>.
- Yaylayan, V.A., 1997. Classification of the Maillard reaction: a conceptual approach. *Trends Food Sci Technol* 8, 13–18. [https://doi.org/10.1016/s0924-2244\(96\)20013-5](https://doi.org/10.1016/s0924-2244(96)20013-5).
- Zheng, J., Ou, J., Ou, S., 2019. Alpha-dicarbonyl compounds. In: Wang, S. (Ed.), *Chemical hazards in thermal-processed foods*. Springer, Nature Singapore Pte Ltd., pp. 19–46.